

Communication-avoiding CholeskyQR2 for rectangular matrices

Edward Hutter and Edgar Solomonik
 Department of Computer Science
 University of Illinois at Urbana-Champaign
 Email: hutter2@illinois.edu and solomon2@illinois.edu

Abstract—

The need for scalable algorithms to solve least squares and eigenvalue problems is becoming increasingly important given the rising complexity of modern machines. We address this concern by presenting a new scalable QR factorization algorithm intended to accelerate these problems for rectangular matrices. Our contribution is a communication-avoiding distributed-memory parallelization of an existing Cholesky-based QR factorization algorithm called CholeskyQR2. Our algorithm exploits a tunable processor grid able to interpolate between one and three dimensions, resulting in tradeoffs in the asymptotic costs of synchronization, horizontal bandwidth, flop count, and memory footprint. It improves the communication cost complexity with respect to state-of-the-art parallel QR implementations by $\Theta(P^{\frac{1}{6}})$. Further, we provide implementation details and performance results on Blue Waters supercomputer. We show that the costs attained are asymptotically equivalent to other communication-avoiding QR factorization algorithms and demonstrate that our algorithm is efficient in practice.

I. INTRODUCTION

The reduced QR factorization, $A = QR$ with orthogonal $Q \in \mathbb{R}^{m \times n}$ and upper-triangular $R \in \mathbb{R}^{n \times n}$, is a ubiquitous subproblem in numerical algorithms for solving linear systems, least squares problems, as well as eigenvalue problems with dense and sparse matrices. In many application contexts, these problems involve very overdetermined systems of equations in a large number of variables, driving a need for scalable parallel QR factorization algorithms. We study communication-efficient algorithms for QR factorizations of rectangular matrices $m \geq n$.

Our work builds on a recently developed algorithm, CholeskyQR2 [1], a Cholesky-based algorithm, designed for tall and skinny matrices. The usual CholeskyQR algorithm computes $\hat{R} \approx R$ as the upper triangular factor in the Cholesky factorization of $n \times n$ matrix $A^T A$, then solves m triangular linear systems of equations, $\hat{Q} = A\hat{R}^{-1}$. The forward error in computing \hat{Q} in CholeskyQR can be as high as $\Theta(\kappa(A)^2)$ where $\kappa(A)$ is the condition number of A . On the other hand, the triangular solves can be done backward stably, so $\hat{Q}\hat{R} = A + \delta A$ with $\|\delta A\| = O(\epsilon)$ where ϵ is the relative error in the machine floating point representation. Therefore, when under effect of round-off error, CholeskyQR computes the factorization of A into a product of a near-orthogonal matrix \hat{Q} and a triangular matrix \hat{R} .

CholeskyQR2 provides a correction to the orthogonal factor by running CholeskyQR once more on \hat{Q} itself, to obtain $Q\delta R = \hat{Q}$ where δR is upper-triangular and near identity, then updating the upper-triangular factor as $R = \delta R\hat{R}$. If \hat{Q} was computed to within a few digits of accuracy, which is guaranteed if $\kappa(A) = O(\sqrt{1/\epsilon})$, it is close to orthogonal and therefore well-conditioned, so the CholeskyQR of \hat{Q} will not lose much precision from round-off error and the QR factorization given by CholeskyQR2 will retain all or nearly all digits of accuracy [2].

A key advantage of CholeskyQR2 is its practicality. It requires only matrix multiplications and Cholesky factorizations. In previous work [3], a 1D parallelization of the algorithm was shown to provide minimal communication cost and synchronization (a logarithmic factor less than other communication-avoiding algorithms [4]). Consequently, the algorithm is of high practical interest for a wide class sufficiently well-conditioned least squares problems. In this work, we extend the algorithm to a 3D parallelization suitable for matrices with arbitrary dimensions.

To construct a scalable CholeskyQR2 algorithm, we must utilize efficient parallel algorithms for Cholesky factorization and matrix multiplication. Much focus has been given to theoretical analysis of the communication cost of matrix multiplication and Gaussian elimination algorithms. We present a simple adaptation of the algorithm therein [5] to Cholesky factorization. Tradeoffs between synchronization and bandwidth are investigated using a tunable parameter, α , representing the depth of recursion. This parameter thus determines the size of the diagonal submatrices. We focus on minimizing bandwidth cost given unbounded memory so we choose to use the value $\alpha = \frac{2}{3}$.

Of the QR algorithms that achieve asymptotically minimal communication, none have been implemented in practice. The use of recursive slanted panels [6] provides a 3D algorithm that is communication efficient for square matrices. Recent work has extended the algorithm to rectangular matrices by using it as a subroutine in the TSQR algorithm for tall and skinny matrices [7]. This algorithm achieves as little communication for rectangular matrices as a matrix multiplication of corresponding dimensions. However, neither slanted-panel based approach is known to have been evaluated in practical performance.

As such, no current QR factorization algorithm that achieves optimal communication cost theoretically has been demonstrated to be practical. Existing algorithms face challenges in their complexity, high constants, and incompatibility with BLAS-like routines. Previously studied parallel CholeskyQR2 algorithms do not scale for matrices of an arbitrary size. The novelty of our communication-avoiding CholeskyQR2 algorithm lies in the combination of its simplicity and asymptotic efficiency. It relies upon a tunable processor grid to ensure optimally minimal communication for matrices of any size while being relatively easy to implement. Our contributions are to provide a detailed specification, cost analysis, implementation, and performance evaluation of the newly proposed algorithm.

II. FOUNDATION AND PREVIOUS WORK

To study the scalability of parallel QR factorization algorithms, we will use the lens of communication cost analysis. In this section, we will introduce results necessary for our work, and provide brief summaries of related work. We first consider collective communication and the parallel algorithms we use for matrix multiplication and Cholesky factorization.

A. Preliminaries

In presenting these algorithms and analyzing their costs, we use a simple α - β - γ model as defined below.

$\alpha \rightarrow$ cost of sending or receiving a single message

$\beta \rightarrow$ cost of moving a single word of data among processors

$\gamma \rightarrow$ cost of computing a single floating point operation

Our analysis assumes $\alpha \gg \beta \gg \gamma$, which is reflective of current parallel computer architectures.

We define a few sequential routines and give their asymptotic costs [8].

$$\begin{aligned} C \leftarrow aX + Y : T_{\text{axpy}}^{\alpha-\beta}(m, n) &= mn \cdot \gamma \\ C \leftarrow \mathbf{MM}(A, B) = AB : T_{\text{MM}}^{\alpha-\beta}(m, n, k) &= 2mnk \cdot \gamma \\ C \leftarrow \mathbf{Syrk}(A) = AA^T : T_{\text{syrk}}^{\alpha-\beta}(m, n) &= mn^2 \cdot \gamma \\ L \leftarrow \mathbf{Chol}(A) : T_{\text{Chol}}^{\alpha-\beta}(n) &= (n^3/3) \cdot \gamma \end{aligned}$$

We also want to define a unit-step function as follows:

$$\delta(x) = \begin{cases} 0 & x \leq 1 \\ 1 & x > 1 \end{cases}.$$

B. Processor Grids and Collective Communication

Collective communication serves as an efficient way to move data among processors over some subset of a processor grid. We partition the processor grid into slices, rows, and columns, among other subdivisions, by splitting communicators into subcommunicators. We define a 3D processor grid Π containing P processors. $\Pi[\mathbf{x}, \mathbf{y}, \mathbf{z}]$ uniquely identifies

every processor in the grid, where each of the \mathbf{x} , \mathbf{y} , and \mathbf{z} dimensions are of size $P^{\frac{1}{3}}$ and $\mathbf{x}, \mathbf{y}, \mathbf{z} \in [0, P^{\frac{1}{3}} - 1]$. Π can be split into 2D slices such as $\Pi[:, :, \mathbf{z}]$, row communicators such as $\Pi[:, \mathbf{y}, \mathbf{z}]$, column communicators such as $\Pi[\mathbf{x}, :, \mathbf{z}]$, and depth communicators such as $\Pi[\mathbf{x}, \mathbf{y}, :]$.

Allgather, Allreduce, and Broadcast are collectives used heavily in the multiplication and factorization algorithms explored below. As these are well known [9]–[13], we give only the function signature and a brief description of each. We assume butterfly network collectives for analysis [10].

- **Transpose**($A, \Pi[\mathbf{y}, \mathbf{x}, \mathbf{z}]$) — all processors $\Pi[\mathbf{x}, \mathbf{y}, \mathbf{z}]$ swap local array A with processor $\Pi[\mathbf{y}, \mathbf{x}, \mathbf{z}]$ via point-to-point communication.
- **Bcast**($A, B, r, \Pi[:, \mathbf{y}, \mathbf{z}]$) — root processor $\Pi[r, \mathbf{y}, \mathbf{z}]$ distributes local array A to every processor in $\Pi[:, \mathbf{y}, \mathbf{z}]$ as local array B .
- **Reduce**($A, B, r, \Pi[\mathbf{x}, :, \mathbf{z}]$) — all processors in $\Pi[\mathbf{x}, :, \mathbf{z}]$ contribute local arrays A to an element-wise reduction onto root processor $\Pi[r, \mathbf{x}, \mathbf{z}]$.
- **Allreduce**($A, B, \Pi[\mathbf{x}, :, \mathbf{z}]$) — all processors in $\Pi[\mathbf{x}, :, \mathbf{z}]$ contribute local arrays A to an element-wise reduction onto some root. The reduced array is then broadcasted into local array B .
- **Allgather**($A, B, \Pi[\mathbf{x}, \mathbf{y}, :]$) — all processors in $\Pi[\mathbf{x}, \mathbf{y}, :]$ contribute local arrays A to a concatenation onto some root. The concatenated array is then broadcasted into local array B .

The costs of the following collective routines can be obtained by a butterfly schedule, where n is the number of words of data being moved and P is the number of processors involved in the communication.

$$\begin{aligned} T_{\text{Transp}}^{\alpha-\beta}(n, P) &= \delta(P) (\alpha + n \cdot \beta) \\ T_{\text{Bcast}}^{\alpha-\beta}(n, P) &= 2 \log_2 P \cdot \alpha + 2n\delta(P) \cdot \beta \\ T_{\text{Reduce}}^{\alpha-\beta}(n, P) &= \log_2 P \cdot \alpha + n\delta(P) \cdot \beta \\ T_{\text{Allreduce}}^{\alpha-\beta}(n, P) &= 2 \log_2 P \cdot \alpha + 2n\delta(P) \cdot \beta \\ T_{\text{Allgather}}^{\alpha-\beta}(n, P) &= \log_2 P \cdot \alpha + n\delta(P) \cdot \beta \end{aligned}$$

We disregard the computational cost in reductions by the assumption $\beta \gg \gamma$.

C. Matrix Multiplication

Matrix multiplication $C = AB$ over Π and other cubic partitions of Π is an important building block for the 3D-CQR2 and CA-CQR2 algorithms presented below. We use a variant of 3D matrix multiplication (which we refer to as 3D SUMMA) that achieves asymptotically optimal communication cost over a 3D processor grid [14]–[19]. Our algorithm MM3D is a customization with respect to known algorithms. First, B is not distributed across $\Pi[P^{\frac{2}{3}} - 1, :, :]$ and is instead distributed across $\Pi[:, :, 0]$ with A . Second, instead of distributing matrix C across $\Pi[:, 0, :]$, we Allreduce C

onto $\Pi[:, :, \mathbf{z}], \forall \mathbf{z} \in [0, P^{\frac{1}{3}} - 1]$ so that each xy slice holds a distributed copy. These differences are motivated by the need for C to be replicated over Π in our new algorithms. 3D SUMMA would require an unnecessary broadcast from $\Pi[:, 0, :]$ to $\Pi[:, :, :]$. A cyclic distribution is used as it is required by our 3D Cholesky factorization algorithm detailed below. See Algorithm 1 for specific details.

Algorithm 1 $[\Pi\langle C \rangle] \leftarrow \text{MM3D}(\Pi\langle A \rangle, \Pi\langle B \rangle, \Pi)$

Require: Π has P processors arranged in a $P^{1/3} \times P^{1/3} \times P^{1/3}$ grid. Matrices A and B are replicated on $\Pi[:, :, \mathbf{z}], \forall \mathbf{z} \in [0, P^{\frac{1}{3}} - 1]$. Each processor $\Pi[\mathbf{x}, \mathbf{y}, \mathbf{z}]$ owns a cyclic partition of $m \times n$ matrix A and $n \times k$ matrix B , referred to as local matrices $\Pi\langle A \rangle$ and $\Pi\langle B \rangle$, respectively. Let X , Y , and Z be temporary arrays with the same distribution as A and B .

- 1: **Bcast** $(\Pi\langle A \rangle, \Pi\langle X \rangle, \mathbf{z}, \Pi[\mathbf{x}, :, \mathbf{z}])$
- 2: **Bcast** $(\Pi\langle B \rangle, \Pi\langle Y \rangle, \mathbf{z}, \Pi[:, \mathbf{y}, \mathbf{z}])$
- 3: $\Pi\langle Z \rangle \leftarrow \text{MM}(\Pi\langle X \rangle, \Pi\langle Y \rangle)$
- 4: **Allreduce** $(\Pi\langle Z \rangle, \Pi\langle C \rangle, \Pi[\mathbf{x}, \mathbf{y}, :])$

Ensure: $C = AB$, where C is $m \times k$ and distributed the same way as A and B .

We analyze the cost of MM3D for multiplying an $m \times n$ matrix by a $n \times k$ matrix in Table I.

Table I: Costs for each line of MM3D algorithm.

| # | Cost |
|---|--|
| 1 | $T_{\text{Bcast}}^{\alpha-\beta}(mk/P^{2/3}, P^{1/3})$ |
| 2 | $T_{\text{Bcast}}^{\alpha-\beta}(nk/P^{2/3}, P^{1/3})$ |
| 3 | $T_{\text{MM}}^{\alpha-\beta}(m, n, k)$ |
| 4 | $T_{\text{Allreduce}}^{\alpha-\beta}(mn/P^{2/3}, P^{1/3})$ |

$$T_{\text{MM3D}}^{\alpha-\beta}(m, n, k, P) = 6 \log_2 P^{\frac{1}{3}} \cdot \alpha + \frac{2(mn + nk + mk) \delta(P)}{P^{2/3}} \cdot \beta + \frac{2mnk}{P} \cdot \gamma$$

D. Cholesky Factorization

Assuming A is a dense, symmetric positive definite matrix of dimension n , the factorization $A = LL^T$ can be expanded into matrix multiplication of submatrices of dimension $n/2$ [5], [20].

$$\begin{bmatrix} A_{11} & A_{21} \\ A_{21} & A_{22} \end{bmatrix} = \begin{bmatrix} L_{11} & L_{21} \\ L_{21} & L_{22} \end{bmatrix} \begin{bmatrix} L_{11}^T & L_{21}^T \\ L_{21}^T & L_{22}^T \end{bmatrix}$$

$$A_{11} = L_{11}L_{11}^T, \quad A_{21} = L_{21}L_{11}^T,$$

$$A_{22} = L_{21}L_{21}^T + L_{22}L_{22}^T$$

These recursive algorithm yields a family of parallel algorithm variants [21]. Rewriting these equations gives a recursive definition for $L \leftarrow \text{Chol}(A)$.

$$L_{11} \leftarrow \text{Chol}(A_{11}), \quad L_{21} \leftarrow A_{21}L_{11}^{-T},$$

$$L_{22} \leftarrow \text{Chol}(A_{22} - L_{21}L_{21}^T)$$

We augment the recursive definition of the Cholesky factorization, using the recursive definition for $Y = L^{-1}$, as motivated by other parallel algorithms leveraging the triangular inverse [5], [22]. Like before, the factorization $I = LY$ gets expanded into matrix multiplication of submatrices of dimension $n/2$.

$$\begin{bmatrix} I & 0 \\ 0 & I \end{bmatrix} = \begin{bmatrix} L_{11} & \\ L_{21} & L_{22} \end{bmatrix} \begin{bmatrix} Y_{11} & Y_{21} \\ Y_{21} & Y_{22} \end{bmatrix}$$

$$I = L_{11}Y_{11}, \quad I = L_{22}Y_{22}, \quad 0 = L_{21}Y_{11} + L_{22}Y_{21}$$

Rewriting these equations gives a recursive definition for $Y \leftarrow \text{Inv}(L)$.

$$Y_{11} \leftarrow \text{Inv}(L_{11}), \quad Y_{22} \leftarrow \text{Inv}(L_{22}), \quad Y_{21} \leftarrow -Y_{22}L_{21}Y_{11}$$

We embed the two recursive definitions and arrive at an algorithm to solve for both the Cholesky factorization of A and the triangular inverse of L . Note that the addition of solving for L^{-1} adds only two extra matrix multiplications at each recursive level to the recursive definition for $A = LL^T$, thus achieving the same asymptotic cost. If L^{-1} were to be solved recursively at each level, the synchronization cost would incur an extra logarithmic factor. We address the missing base case in the cost analysis derivation below.

Algorithm 2 $[L, Y] \leftarrow \text{CholInv}(A)$

Require: A is a symmetric matrix of dimension n .

- 1: if $n = 1$ return $L = A, Y = A^{-1}$
- 2: $L_{11}, Y_{11} \leftarrow \text{CholInv}(A_{11})$
- 3: $L_{21} \leftarrow A_{21}Y_{11}^T$
- 4: $L_{22}, Y_{22} \leftarrow \text{CholInv}(A_{22} - L_{21}L_{21}^T)$
- 5: $L \leftarrow \begin{bmatrix} L_{11} & \\ L_{21} & L_{22} \end{bmatrix}$
- 6: $Y \leftarrow \begin{bmatrix} Y_{11} & \\ -Y_{22}L_{21}Y_{11} & Y_{22} \end{bmatrix}$

Require: L is lower triangular, $A = LL^T$.

We incorporate two matrix transposes at each recursive level to take into account L_{11}^{-T} and L_{21}^T needed in the equations above. Processor $\Pi[\mathbf{x}, \mathbf{y}, \mathbf{z}], \forall \mathbf{z} \in [0, P^{\frac{1}{3}} - 1]$ must send its local data to $\Pi[\mathbf{y}, \mathbf{x}, \mathbf{z}]$ to transpose the matrix globally. A local transpose without horizontal communication will yield an incorrect distributed transpose.

A cyclic distribution of the matrices among processors $\Pi[:, :, \mathbf{z}], \forall \mathbf{z} \in [0, P^{\frac{1}{3}} - 1]$ is chosen to utilize every processor in the recursive calls performed on submatrices. Upon reaching the base case where matrix dimension $n = n_o$, the square region of the matrix is scattered over the $P^{\frac{1}{3}}$ processors encompassing $\Pi[:, :, \mathbf{z}], \forall \mathbf{z} \in [0, P^{\frac{1}{3}} - 1]$ and an Allgather must be performed to load the region onto each. After all P processors perform a Cholesky factorization and triangular inverse, each stores only the data it owns according to the cyclic rule. See Algorithm 3 for full details.

Algorithm 3 $[\Pi\langle L \rangle, \Pi\langle Y \rangle] \leftarrow \mathbf{CFR3D}(\Pi\langle A \rangle, n_o, \Pi)$

Require: Π has P processors arranged in a $P^{1/3} \times P^{1/3} \times P^{1/3}$ 3D grid. Matrix A is of dimension n , symmetric, and positive definite. A is replicated on $\Pi[:, :, \mathbf{z}]$, $\forall \mathbf{z} \in [0, P^{\frac{1}{3}} - 1]$. Each processor $\Pi[\mathbf{x}, \mathbf{y}, \mathbf{z}]$ owns a cyclic partition of A given by $\Pi\langle A \rangle$. Let T , W , X , U , and Z be temporary arrays, distributed the same way as A .

```

1: if  $n = n_o$  then
2:   Allgather( $\Pi\langle A \rangle, T, \Pi[:, :, \mathbf{z}]$ )
3:    $L, Y \leftarrow \mathbf{CholInv}(T, n)$ 
4: else
5:    $\Pi\langle L_{11} \rangle, \Pi\langle Y_{11} \rangle \leftarrow \mathbf{CFR3D}(\Pi\langle A_{11} \rangle, n_o, \Pi)$ 
6:    $\Pi\langle W \rangle \leftarrow \mathbf{Transpose}(\Pi\langle Y_{11} \rangle, \Pi[\mathbf{y}, \mathbf{x}, \mathbf{z}])$ 
7:    $\Pi\langle L_{21} \rangle \leftarrow \mathbf{MM3D}(\Pi\langle A_{21} \rangle, \Pi\langle W \rangle^T, \Pi)$ 
8:    $\Pi\langle X \rangle \leftarrow \mathbf{Transpose}(\Pi\langle L_{21} \rangle, \Pi[\mathbf{y}, \mathbf{x}, \mathbf{z}])$ 
9:    $\Pi\langle U \rangle \leftarrow \mathbf{MM3D}(\Pi\langle L_{21} \rangle, \Pi\langle X \rangle^T, \Pi)$ 
10:   $\Pi\langle Z \rangle \leftarrow \Pi\langle A_{22} \rangle - \Pi\langle U \rangle$ 
11:   $\Pi\langle L_{22} \rangle, \Pi\langle Y_{22} \rangle \leftarrow \mathbf{CFR3D}(\Pi\langle Z \rangle, n_o, \Pi)$ 
12:   $\Pi\langle U \rangle \leftarrow \mathbf{MM3D}(\Pi\langle L_{21} \rangle, \Pi\langle Y_{11} \rangle, \Pi)$ 
13:   $\Pi\langle W \rangle \leftarrow -\Pi\langle Y_{22} \rangle$ 
14:   $\Pi\langle Y_{21} \rangle \leftarrow \mathbf{MM3D}(\Pi\langle W \rangle, \Pi\langle U \rangle, \Pi)$ 

```

Ensure: $A = LL^T$, $Y = L^{-1}$, where matrices L and Y are distributed the same way as A .

The cost of CFR3D is determined by the cost of matrix multiplication at each recursive level and the total cost of the base case. In order to utilize the entire 3D processor grid, Π , for each instance of MM3D, we recurse into smaller matrix windows without splitting Π . This influences our decision to use a cyclic distribution because each processor owns an active part of the shrinking matrix window. Upon reaching matrix window size $\frac{n}{2^z} = n_o$, matrices L and L^{-1} are solved explicitly using Cholesky and triangular inversion. An allgather routine is needed to load the data scattered across the matrix window into $\Pi[:, :, \mathbf{z}]$, $\forall \mathbf{z} \in [0, P^{\frac{1}{3}} - 1]$. The combined communication cost of the base case must not dominate the cost of the MM3D.

We analyze the cost of CFR3D in Table II.

Table II: Costs for each line of CFR3D algorithm.

| # | Cost |
|----|---|
| 2 | $T_{\text{Allgather}}^{\alpha-\beta}(n_o^2, P^{2/3})$ |
| 3 | $T_{\text{Chol}}^{\alpha-\beta}(n_o)$ |
| 5 | $T_{\text{CFR3D}}^{\alpha-\beta}(n/2, P)$ |
| 6 | $T_{\text{Transp}}^{\alpha-\beta}(n^2/2, P)$ |
| 7 | $T_{\text{MM3D}}^{\alpha-\beta}(n/2, n/2, n/2, P)$ |
| 8 | $T_{\text{Transp}}^{\alpha-\beta}(n^2/2, P)$ |
| 9 | $T_{\text{MM3D}}^{\alpha-\beta}(n/2, n/2, n/2, P)$ |
| 10 | $T_{\text{axpy}}^{\alpha-\beta}(n^2, P^{2/3})$ |
| 11 | $T_{\text{CFR3D}}^{\alpha-\beta}(n/2, P)$ |
| 12 | $T_{\text{MM3D}}^{\alpha-\beta}(n/2, n/2, n/2, P)$ |
| 14 | $T_{\text{MM3D}}^{\alpha-\beta}(n/2, n/2, n/2, P)$ |

$$\begin{aligned}
T_{\text{BaseCase}}^{\alpha-\beta}(n_o, P) &= \frac{2}{3} \log_2 P \cdot \alpha + n_o^2 \delta(P) \cdot \beta + \frac{4}{3} n_o^3 \cdot \gamma \\
&= \mathcal{O}(\log P \cdot \alpha + n_o^2 \delta(P) \cdot \beta + n_o^3 \cdot \gamma)
\end{aligned}$$

Choice of n_o depends on the non-recursive communication cost. Because $\frac{n}{2^z} = n_o$, our algorithm must compute $\frac{n}{n_o}$ Allgathers.

$$\begin{aligned}
T_{\text{CFR3D}}^{\alpha-\beta}(n, P) &= 2T_{\text{CFR3D}}^{\alpha-\beta}(n/2, P) + (8 \log_2 P + 2\delta(P)) \cdot \alpha \\
&\quad + \frac{(22.5n^2 + 7n) \delta(P)}{4P^{2/3}} \cdot \beta + \frac{n^3}{P} \cdot \gamma \\
&= 2T_{\text{CFR3D}}^{\alpha-\beta}\left(\frac{n}{2}, P\right) + \mathcal{O}\left(\log P \cdot \alpha + \frac{n^2 \delta(P)}{P^{2/3}} \cdot \beta + \frac{n^3}{P} \cdot \gamma\right) \\
&= \mathcal{O}\left(\frac{n \log P}{n_o} \cdot \alpha + n\left(n_o + \frac{n}{P^{\frac{2}{3}}}\right) \delta(P) \cdot \beta + n\left(n_o^2 + \frac{n^2}{P}\right) \cdot \gamma\right)
\end{aligned}$$

Choice of $\frac{n}{n_o}$ creates a tradeoff between the synchronization cost and the communication cost. We elect to match the communication cost at the expense of an increase in synchronization, giving the relation $n_o = \frac{n}{P^{\frac{2}{3}}}$. The final cost of the 3D algorithm is

$$T_{\text{CFR3D}}^{\alpha-\beta}(n, P) = \mathcal{O}\left(P^{2/3} \log P \cdot \alpha + \frac{n^2 \delta(P)}{P^{2/3}} \cdot \beta + \frac{n^3}{P} \cdot \gamma\right).$$

E. QR Factorization

QR factorization decomposes an $m \times n$ matrix A into matrices Q and R such that $A = QR$. We focus on the case when $m \geq n$ and Q and R are the results of a reduced QR factorization. In this case, Q is $m \times n$ with orthonormal columns and R is $n \times n$ and upper-triangular. Parallel QR algorithms have received much study [3], [23]–[28], but focus has predominantly been on 2D blocked algorithms. 3D algorithms for QR have been proposed [6], [7].

Algorithms 4 and 5 give pseudocode for the sequential CholeskyQR2 (CQR2) algorithm. It is composed of matrix multiplications and Cholesky factorizations and unlike other QR factorization algorithms, does not require explicit QR factorizations [1]. Using the building block algorithms explored above, we seek to extend the existing parallel 1D-CQR2 algorithm given in Algorithms 6 and 7 to efficiently handle an arbitrary number of rows and columns.

Algorithm 4 $[Q, R] \leftarrow \mathbf{CQR}(A)$

Require: A is $m \times n$

```

1:  $W \leftarrow \mathbf{Syrk}(A)$ 
2:  $R^T \leftarrow \mathbf{Chol}(W)$ 
3:  $Q \leftarrow \mathbf{MM}(A, R^{-1})$ 

```

Ensure: $A = QR$, where Q is $m \times n$ orthogonal, R is $n \times n$ upper triangular

Algorithm 5 $[Q, R] \leftarrow \mathbf{CQR2}(A)$

Require: A is $m \times n$

- 1: $Q_1, R_1 \leftarrow \mathbf{CQR}(A)$
- 2: $Q, R_2 \leftarrow \mathbf{CQR}(Q_1)$
- 3: $R \leftarrow \mathbf{MM}(R_2, R_1)$

Ensure: $A = QR$, where Q is $m \times n$ orthogonal, R is $n \times n$ upper triangular

F. 1D-CholeskyQR2

The existing parallel 1D-CQR2 algorithm is solved over 1D processor grid Π [1]. It partitions the $m \times n$ matrix A into P rectangular chunks of size $m/P \times n$. The motivation behind this parallelization strategy lies in minimal required communication. Each processor can perform a sequential symmetric rank- m/P update (syrk) with its partition of A , resulting in $n \times n$ matrix $\Pi\langle X \rangle = \Pi\langle A \rangle^T \Pi\langle A \rangle$, $\forall p \in [0, P-1]$. 1D parallelization allows each processor to perform local matrix multiplication with its initial partition of A and contribute to the summation across rows using an allreduce routine. Note that each processor needs only contribute the upper-triangle of each symmetric matrix $\Pi\langle X \rangle$.

Matrix Z is now replicated along all processors. Each processor performs a sequential Cholesky factorization with its copy of Z and solves for R^{-T} . Finally, because Q is distributed in the same manner as A , horizontal communication is not required and each processor can solve for $\Pi\langle Q \rangle$ with $\Pi\langle A \rangle$ and its copy of R^{-1} . See Figure 1 and Algorithm 6 for finer details.

1D-CQR2 calls 1D-CQR twice to solve for Q as shown in Algorithms 5 and 7. Each processor can solve for $R \leftarrow R_2 R_1$ sequentially. This algorithm ensures that Q is distributed the same as A and R is stored on every processor.

To be efficient in practice, n should be small enough to make the Allreduce feasible under given memory constraints. It is most efficient when $m \gg n$. For any given $m \times n$ matrix A , the size and shapes of the local rectangular blocks can be tuned. In general, 1D-CQR2 can only be applied to extremely overdetermined matrices. The 3D-CQR2 and CA-CQR2 algorithms expand 1D-CQR2 to handle matrices of any size.

See Table III for the costs attained in the 1D-CQR algorithm. Note that the Allreduce in line 2 need only send the upper-triangle of symmetric matrix B_p , so a factor of $\frac{1}{2}$ is applied to the horizontal bandwidth cost.

Table III: Costs for each line of 1D-CQR algorithm.

| # | Cost |
|---|---|
| 1 | $T_{\text{syrk}}^{\alpha-\beta}(n, m/P)$ |
| 2 | $T_{\text{Allreduce}}^{\alpha-\beta}(n^2, P)$ |
| 3 | $T_{\text{Chol}}^{\alpha-\beta}(n)$ |
| 4 | $T_{\text{MM}}^{\alpha-\beta}(n, n, m/P)$ |

Algorithm 6 $[\Pi\langle Q \rangle, R] \leftarrow \mathbf{1D-CQR}(\Pi\langle A \rangle, \Pi)$

Require: Π has P processors arranged in a 1D grid. Each processor owns a (cyclic) blocked partition of $m \times n$ input matrix A given by $\Pi\langle A \rangle \in \mathbb{R}^{\frac{m}{P} \times n}$. Let X and Y be temporary arrays.

- 1: $\Pi\langle X \rangle \leftarrow \mathbf{Syrk}(\Pi\langle A \rangle) \quad \triangleright \Pi\langle X \rangle \leftarrow \Pi\langle A \rangle^T \Pi\langle A \rangle$
- 2: $\mathbf{Allreduce}(\Pi\langle X \rangle, Z, \Pi) \quad \triangleright Z \leftarrow A^T A$
- 3: $R^T, R^{-T} \leftarrow \mathbf{CholInv}(Z) \quad \triangleright R^T, R^{-T} \leftarrow Z$
- 4: $\Pi\langle Q \rangle \leftarrow \mathbf{MM}(\Pi\langle A \rangle, R^{-1}) \quad \triangleright Q \leftarrow AR^{-1}$

Ensure: $A = QR$, where Q is distributed the same as A , R is an upper triangular matrix of dimension n owned locally by every processor and packed into a 1D array of size $\frac{n(n+1)}{2}$.

Algorithm 7 $[\Pi\langle Q \rangle, R] \leftarrow \mathbf{1D-CQR2}(\Pi\langle A \rangle, \Pi)$

Require: Same requirements as Algorithm 6.

- 1: $\Pi\langle X \rangle, W \leftarrow \mathbf{1D-CQR}(\Pi\langle A \rangle, \Pi)$
- 2: $\Pi\langle Q \rangle, Z \leftarrow \mathbf{1D-CQR}(X, \Pi)$
- 3: $R \leftarrow \mathbf{MM}(Z, W)$

Ensure: Same requirements as Algorithm 6.

$$T_{\text{1D-CQR}}^{\alpha-\beta}(m, n, P) = 2 \log_2 P \cdot \alpha + n^2 \delta(P) \cdot \beta + \left(\frac{3mn^2}{P} + \frac{1}{3}n^3 \right) \cdot \gamma$$

The costs in Table IV are attained in the 1D-CQR2 algorithm.

Table IV: Costs for each line of 1D-CQR2 algorithm.

| # | Cost |
|---|---|
| 1 | $T_{\text{1D-CQR}}^{\alpha-\beta}(m, n, P)$ |
| 2 | $T_{\text{1D-CQR}}^{\alpha-\beta}(m, n, P)$ |
| 3 | $(1/3)n^3 \cdot \gamma$ |

$$T_{\text{1D-CQR2}}^{\alpha-\beta}(m, n, P) = 4 \log_2 P \cdot \alpha + 2n^2 \delta(P) \cdot \beta + \left(\frac{6mn^2}{P} + n^3 \right) \cdot \gamma$$

This algorithm achieves poor scalability in communication, computation, and memory footprint. Regardless of P , the Allgather distributes an $n \times n$ matrix onto each processor and as n grows the matrix won't fit into a reasonably sized memory. Results from [1] show that this algorithm performs well when $m \gg n$. Therefore, this algorithm can only be used when $m \gg n$. Below, we show that CA-CQR2 can scale efficiently on a tunable processor grid.

III. COMMUNICATION-AVOIDING CHOLESKYQR2

Our main goal is to parallelize Cholesky-QR2 to be scalable when factoring rectangular matrices of arbitrary dimensions $m \geq n$. We start with a 3D algorithm optimized when $m = n$. Matrix A is initially distributed across $\Pi[\cdot, \cdot, z]$, $\forall z \in [0, P^{1/3}-1]$ and is partitioned into rectangular chunks of size $m/P^{1/3} \times n/P^{1/3}$. We compute $Z = A^T A$ in a similar way

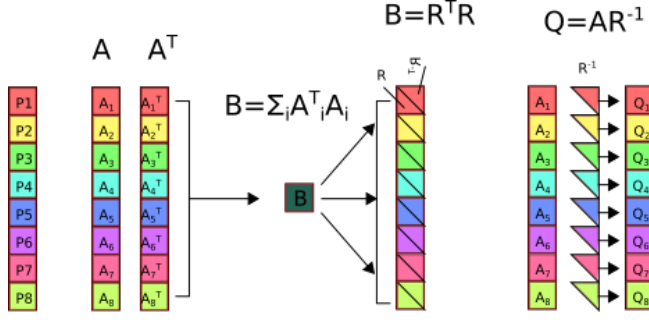


Figure 1: Illustration of each step in the existing parallel 1D-CQR algorithm.

to MM3D. To distribute Z in a 2D layout across $\Pi[:, :, z]$ for each $z \in [0, P^{1/3}-1]$, $\Pi[x, y, z]$ must first receive the sub-matrix $\Pi\langle A \rangle$ from $\Pi[:, :, z]$ as $\Pi\langle W \rangle$. After performing local matrix multiplication with $\Pi\langle W \rangle^T$ and $\Pi\langle A \rangle$, $\Pi[x, y, z]$ completes the global matrix multiplication with a reduction and broadcast. Similar to how the Allreduce in 1D-CQR2 accomplished summing the rows efficiently in parallel, a reduction along $\Pi[x, :, z]$ onto root $z, \forall x, z \in [0, P^{1/3}-1]$ sums the rows of $\Pi\langle X \rangle$. A unique row partition of X is now scattered across Π . A broadcast along $\Pi[x, y, :], \forall x, y \in [0, P^{1/3}-1]$ ensures that $\Pi[:, :, z], \forall z \in [0, P^{1/3}-1]$ owns a copy of Z .

Now that Z is distributed the same as A , CFR3D can solve for R^T over Π . Finally, MM3D solves for Q , which is again distributed the same as A . See Algorithm 8.

3D-CQR2 calls 3D-CQR twice to solve for Q as shown in Algorithm 5 and 7. MM3D is invoked over Π to solve $R \leftarrow R_2 R_1$. This algorithm ensures that Q and R are distributed the same as A . See Algorithm 9.

Algorithm 8 $[\Pi\langle Q \rangle, \Pi\langle R \rangle] \leftarrow \mathbf{3D-CQR}(\Pi\langle A \rangle, \Pi)$

Require: Π has P processors arranged in a 3D grid. A is $m \times n$ and is replicated on $\Pi[:, :, z], \forall z \in [0, P^{1/3}-1]$. Each processor $\Pi[x, y, z]$ owns a (cyclic) blocked partition of A given by $\Pi\langle A \rangle \in \mathbb{R}^{m/P^{1/3} \times n/P^{1/3}}$. Let W, X, Y, Z , and R^{-1} be temporary arrays distributed the same as A .

- 1: **Bcast**($\Pi\langle A \rangle, \Pi\langle W \rangle, z, \Pi[:, y, z]$)
- 2: $\Pi\langle X \rangle \leftarrow \mathbf{MM}(\Pi\langle W \rangle^T, \Pi\langle A \rangle)$
- 3: **Reduce**($\Pi\langle X \rangle, \Pi\langle Y \rangle, z, \Pi[x, :, z]$)
- 4: **Bcast**($\Pi\langle Y \rangle, \Pi\langle Z \rangle, y, \Pi[x, y, :]$)
- 5: $\Pi\langle R^T \rangle, \Pi\langle R^{-T} \rangle \leftarrow \mathbf{CFR3D}(\Pi\langle Z \rangle, \Pi)$
- 6: $\Pi\langle Q \rangle \leftarrow \mathbf{MM3D}(\Pi\langle A \rangle, \Pi\langle R^{-1} \rangle, \Pi)$

Ensure: $A = QR$, where Q and R are distributed the same as A . Q is $m \times n$ and R is an upper triangular matrix of dimension n .

The costs in Table V are attained in the 3D-CQR algorithm.

Table V: Costs for each line of 3D-CQR algorithm.

Algorithm 9 $[\Pi\langle Q \rangle, \Pi\langle R \rangle] \leftarrow \mathbf{3D-CQR2}(\Pi\langle A \rangle, \Pi)$

Require: Same requirements as Algorithm 8.

- 1: $\Pi\langle X \rangle, \Pi\langle Y \rangle \leftarrow \mathbf{3D-CQR}(\Pi\langle A \rangle, \Pi)$
- 2: $\Pi\langle Q \rangle, \Pi\langle Z \rangle \leftarrow \mathbf{3D-CQR}(\Pi\langle X \rangle, \Pi)$
- 3: $\Pi\langle R \rangle \leftarrow \mathbf{MM3D}(\Pi\langle Z \rangle, \Pi\langle Y \rangle, \Pi)$

Ensure: Same requirements as Algorithm 8.

| # | Cost |
|---|---|
| 1 | $T_{\text{Bcast}}^{\alpha-\beta}(mn/P^{2/3}, P^{1/3})$ |
| 2 | $T_{\text{MM}}^{\alpha-\beta}(\frac{n}{P^{1/3}}, \frac{n}{P^{1/3}}, \frac{m}{P^{1/3}})$ |
| 3 | $T_{\text{Reduce}}^{\alpha-\beta}(\frac{n^2}{P^{2/3}}, P^{1/3})$ |
| 4 | $T_{\text{Bcast}}^{\alpha-\beta}(\frac{n^2}{P^{2/3}}, P^{1/3})$ |
| 5 | $T_{\text{CFR3D}}^{\alpha-\beta}(n, P)$ |
| 6 | $T_{\text{MM3D}}^{\alpha-\beta}(m, n, n, P)$ |

$$T_{\text{3D-CQR}}^{\alpha-\beta}(m, n, P) = \mathcal{O}\left(P^{2/3} \log P \cdot \alpha + \frac{mn\delta(P)}{P^{2/3}} \cdot \beta + \frac{mn^2}{P} \cdot \gamma\right)$$

The costs in Table VI are attained in the 3D-CQR2 algorithm.

Table VI: Costs for each line of 3D-CQR2 algorithm.

| # | Cost |
|---|--|
| 1 | $T_{\text{3D-CQR}}^{\alpha-\beta}(m, n, P)$ |
| 2 | $T_{\text{3D-CQR}}^{\alpha-\beta}(m, n, P)$ |
| 3 | $2 \log_2 P \cdot \alpha + \frac{(3n^2 + 6nP^{1/3})\delta(P)}{2P^{2/3}} \cdot \beta + \frac{n^3}{3P} \cdot \gamma$ |

$$T_{\text{3D-CQR2}}^{\alpha-\beta}(m, n, P) = \mathcal{O}\left(P^{2/3} \log P \cdot \alpha + \frac{mn\delta(P)}{P^{2/3}} \cdot \beta + \frac{mn^2}{P} \cdot \gamma\right)$$

This algorithm is most communication efficient when $m = n$.

For problems like QR factorization that solve or factor rectangular matrices, tunable processor grids have several advantages over static grids. They can act as shapeshifters, able to imitate the shape of the matrix and tune themselves to optimize certain parameters such as memory size and horizontal communication. Tunable algorithms solved over tunable grids can achieve a wide range of asymptotic costs. These costs can be shown to interpolate between known algorithms on specific grids. Reduced communication is only possible when the correct processor grid is utilized. Skinny matrices can not take full advantage of the resources provided by a 3D grid, while square matrices overload the resource capacity that skinny rectangular grids provide. Finding the optimal processor grid for a specific algorithm is nontrivial.

The CA-CQR2 algorithm can be seen as a generalization of 1D-CQR2 and 3D-CQR2. We define a $c \times d \times c$ rectangular processor grid Π that partitions the $m \times n$ matrix A into rectangular blocks of size $\frac{m}{d} \times \frac{n}{c}$. CA-CQR2 effectively utilizes its tunable grid by performing $\frac{d}{c}$ simultaneous instances of CFR3D on cubic grid partitions of dimension c . This allows each grid partition to avoid further communication with other partitions because each has the necessary data to compute the final step $Q = AR^{-1}$. In order to allow these simultaneous Cholesky factorizations, a few extra steps are needed to get the required data onto the correct processor.

As in 3D-CQR, $\Pi[\mathbf{z}, \mathbf{y}, \mathbf{z}]$ broadcasts $\Pi\langle A \rangle$ to $\Pi[\mathbf{z}, \mathbf{y}, \mathbf{z}], \forall \mathbf{y} \in [0, d-1], \mathbf{z} \in [0, c-1]$. With its received data and local data, each processor can perform matrix multiplication $\Pi\langle X \rangle \leftarrow \Pi\langle W \rangle^T \Pi\langle A \rangle$. In order for c cubic partitions of Π to own the same matrix $Z = A^T A$, we perform the following two steps. First, we subdivide Π along dimension y into $\frac{d}{c}$ contiguous groups of size c . Each group participates in an Allreduce in order to simulate the horizontal summing of rows in a linear combination. Processor $\Pi[\mathbf{x}, \mathbf{y}, \mathbf{z}], \forall \mathbf{x}, \mathbf{z} \in [0, c-1], \forall \mathbf{y}$ such that $\mathbf{y} \bmod c = \mathbf{z}$ for its corresponding z dimension index \mathbf{z} , is the only processor that must retain the communicated data. To get the data from the other $\frac{d}{c}-1$ groups on each slice, we subdivide Π along dimension y into c groups of size $\frac{d}{c}$, where each processor belonging to the same group is a step size c away. The Allreduce is performed on subcommunicator $\Pi[\mathbf{x}, 0 : c : d, \mathbf{z}], \forall \mathbf{x}, \mathbf{z} \in [0, c-1], \forall \mathbf{y} = \mathbf{z}$ on dimension- z index \mathbf{z} , resulting in every processor in that subcommunicator owning the correct region of $B = A^T A$. A final broadcast from root $\Pi[\mathbf{x}, \mathbf{y}, \mathbf{z}], \forall \mathbf{x}, \mathbf{z} \in [0, c-1], \forall \mathbf{y}$ such that $\mathbf{y} \bmod c = \mathbf{z}$ for its corresponding z dimension index \mathbf{z} , along $\Pi[\mathbf{x}, \mathbf{y}, :], \forall \mathbf{x} \in [0, c-1], \mathbf{y} \in [0, d-1]$ ensures that B is replicated $\frac{d}{c} \cdot c$ times among subcommunicators of size c^2 .

Now that Z is distributed as described above, $\frac{d}{c}$ simultaneous instances of CFR3D and MM3D are performed over Π_{subcube} . CA-CQR2 requires calling CA-CQR twice and performing a final MM3D to solve for R .

As evidenced by Figure 2 and the pseudocode presented in Algorithms 10 and 11, CA-CQR2 combines elements of both the 1D-CQR2 and 3D-CQR2 algorithms in order to most efficiently span the grid range $c \in [1, P^{1/3}]$. To prove that this algorithm achieves the same costs as 1D-CQR2 and 3D-CQR2 with grid sizes $c = 1, c = P^{1/3}$, respectively, we provide a cost analysis below.

Algorithm 10 $[\Pi\langle Q \rangle, \Pi\langle R \rangle] \leftarrow \text{CA-CQR}(\Pi\langle A \rangle, \Pi)$

Require: Π has P processors arranged in a tunable grid of size $c \times d \times c$ for any integer c in range $[0, P^{1/3}-1]$. A is $m \times n$ and is replicated on $\Pi[\mathbf{z}, :, \mathbf{z}], \forall \mathbf{z} \in [0, c-1]$. Each processor $\Pi[\mathbf{x}, \mathbf{y}, \mathbf{z}]$ owns a (cyclic) blocked partition of A given by $\Pi\langle A \rangle \in \mathbb{R}^{\frac{m}{d} \times \frac{n}{c}}$. Let W, X, Y, Z , and R^{-1} be temporary arrays distributed the same as A .

- 1: **Bcast** $(\Pi\langle A \rangle, \Pi\langle W \rangle, \mathbf{z}, \Pi[\mathbf{z}, \mathbf{y}, \mathbf{z}])$
- 2: $\Pi\langle X \rangle \leftarrow \text{MM}(\Pi\langle W \rangle^T, \Pi\langle A \rangle)$
- 3: **Reduce** $(\Pi\langle X \rangle, \Pi\langle Y \rangle, c[\mathbf{y}/c], \Pi[\mathbf{x}, c[\mathbf{y}/c] : c[\mathbf{y}/c], \mathbf{z}])$:
- 4: **Allreduce** $(\Pi\langle Y \rangle, \Pi\langle Z \rangle, \Pi[\mathbf{x}, 0 : c : d, \mathbf{z}])$
- 5: **Bcast** $(\Pi\langle Z \rangle, \Pi\langle Z \rangle, \mathbf{z}, \Pi[\mathbf{x}, \mathbf{y}, :])$
- 6: Define $\Pi_{\text{subcube}}[\mathbf{x}, \mathbf{y}, \mathbf{z}] \leftarrow \Pi[\mathbf{x}, c[\mathbf{y}/c] : c[\mathbf{y}/c], \mathbf{z}]$
- 7: $\Pi\langle R^T \rangle, \Pi\langle R^{-T} \rangle \leftarrow \text{CFR3D}(\Pi\langle Z \rangle, \Pi_{\text{subcube}})$
- 8: $\Pi\langle Q \rangle \leftarrow \text{MM3D}(\Pi\langle A \rangle, \Pi\langle R^{-1} \rangle, \Pi_{\text{subcube}})$

Ensure: $A = QR$, where Q and R are distributed the same as A . Q is $m \times n$ and R is an upper triangular matrix of dimension n .

Algorithm 11 $[\Pi\langle Q \rangle, \Pi\langle R \rangle] \leftarrow \text{CA-CQR2}(\Pi\langle A \rangle, \Pi)$

Require: Same requirements as Algorithm 10.

- 1: $\Pi\langle X \rangle, \Pi\langle Y \rangle \leftarrow \text{CA-CQR}(\Pi\langle A \rangle, \Pi)$
- 2: $\Pi\langle Q \rangle, \Pi\langle Z \rangle \leftarrow \text{CA-CQR}(\Pi\langle X \rangle, \Pi)$
- 3: Define $\Pi_{\text{subcube}}[\mathbf{x}, \mathbf{y}, \mathbf{z}] \leftarrow \Pi[\mathbf{x}, c[\mathbf{y}/c] : c[\mathbf{y}/c], \mathbf{z}]$
- 4: $\Pi\langle R \rangle \leftarrow \text{MM3D}(\Pi\langle Z \rangle, \Pi\langle Y \rangle, \Pi_{\text{subcube}})$

Ensure: Same requirements as Algorithm 10.

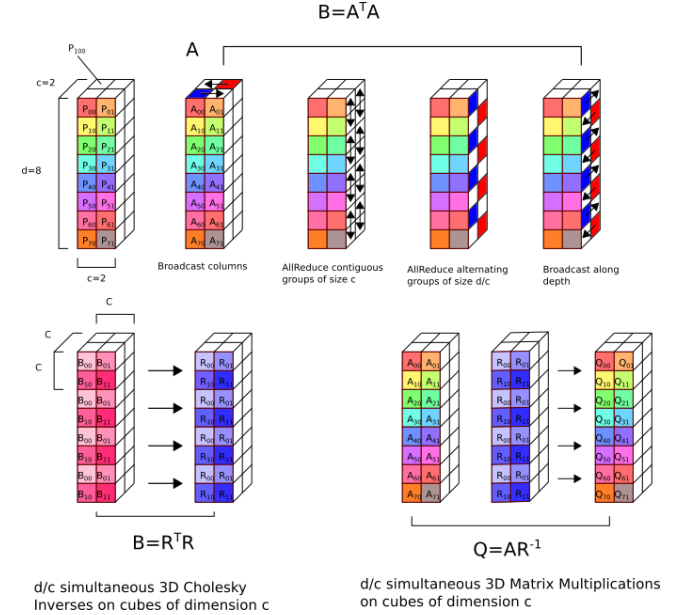


Figure 2: Illustration of the steps required to perform CQR over a tunable processor grid.

The CA-CQR algorithm attains the costs in Table VII.

Table VII: Costs for each line of CA-CQR algorithm.

| # | Cost |
|---|---|
| 1 | $T_{\text{Bcast}}^{\alpha-\beta}(\frac{mn}{dc}, c)$ |
| 2 | $T_{\text{MM}}^{\alpha-\beta}(n/c, n/c, m/d)$ |
| 3 | $T_{\text{Reduce}}^{\alpha-\beta}(n^2/c^2, c)$ |
| 4 | $T_{\text{Allreduce}}^{\alpha-\beta}(n^2/c^2, d/c)$ |
| 5 | $T_{\text{Bcast}}^{\alpha-\beta}(\frac{mn}{dc}, c)$ |
| 7 | $T_{\text{CFR3D}}^{\alpha-\beta}(n, c^3)$ |
| 8 | $T_{\text{MM3D}}^{\alpha-\beta}(m, n, n, P)$ |

$$\begin{aligned}
T_{\text{CA-CQR}}^{\alpha-\beta}(m, n, c, d) &= \mathcal{O}\left(\left(c^2 \log c + \log \frac{d}{c}\right) \cdot \alpha \right. \\
&\quad \left. + \left(\frac{mn\delta(c)}{dc} + \frac{n^2\delta(P)}{c^2}\right) \cdot \beta + \left(\frac{n^3}{c^3} + \frac{mn^2}{c^2d}\right) \cdot \gamma\right) \\
&= \mathcal{O}\left(c^2 \log P \cdot \alpha + \frac{cmn\delta(c) + n^2d\delta(P)}{dc^2} \cdot \beta \right. \\
&\quad \left. + \frac{n^3d + mn^2c}{c^3d} \cdot \gamma\right)
\end{aligned}$$

See Table VIII for the costs attained in the CA-CQR2 algorithm.

| | | | |
|-----------------------|-----------------------|---|-----------------------|
| $c \times d \times c$ | $1 \times P \times 1$ | $P^{\frac{1}{3}} \times P^{\frac{1}{3}} \times P^{\frac{1}{3}}$ | optimal |
| # of msgs | $\log P$ | $P^{2/3} \log P$ | $(Pn/m)^{2/3} \log P$ |
| # of words | n^2 | $mn/P^{2/3}$ | $(mn^2/P)^{2/3}$ |
| # of flops | mn^2/P | mn^2/P | mn^2/P |
| # mem use | $mn/P + n^2$ | $mn/P^{2/3}$ | $(mn^2/P)^{2/3}$ |

Table IX: Asymptotic complexity of CholeskyQR2 algorithm in terms of latency cost (msgs), bandwidth cost (words), computational cost (flops), and memory foot print (mem use).

Table VIII: Costs for each line of CA-CQR2 algorithm.

| # | Cost |
|---|--|
| 1 | $T_{\text{CA-CQR}}^{\alpha-\beta}(m, n, c, d)$ |
| 2 | $T_{\text{CA-CQR}}^{\alpha-\beta}(m, n, c, d)$ |
| 3 | $T_{\text{MM3D}}^{\alpha-\beta}(n, n, n, c^3)$ |

$$T_{\text{CA-CQR2}}^{\alpha-\beta}(m, n, c, d) = \mathcal{O}\left(c^2 \log P \cdot \alpha + \frac{mn\delta(c)}{dc} \cdot \beta + \frac{mn^2}{c^2 d} \cdot \gamma\right)$$

We can show that costs attained by CA-CQR2 correctly interpolate between the costs of 1D-CQR2 and 3D-CQR2. Note that our $c \times d \times c$ grid requires $P = c^2 d$ and $d \geq c$.

$$T_{\text{CA-CQR2}}^{\alpha-\beta}(m, n, P^{1/3}, P^{1/3}) = \mathcal{O}\left(P^{2/3} \log P \cdot \alpha + \frac{mn\delta(P)}{P^{2/3}} \cdot \beta + \frac{mn^2}{P} \cdot \gamma\right)$$

The advantage of using a tunable grid lies in the ability to frame the shape of the grid around the shape of rectangular $m \times n$ matrix A . If $m \gg n$, it might make sense to let $c = 1$, giving a 1D grid of shape $1 \times P \times 1$ on which we can run 1D-CQR2. If $m = n$, it might be most performant to allow $c = P^{1/3}$, producing a cubic grid of dimensions $P^{1/3}$. If A is between these shapes, our tunable grid can factor $A = QR$ at asymptotically less cost. Optimal communication can be attained by ensuring that the grid perfectly fits the dimensions of A , or that the dimensions of the grid are proportional to the dimensions of the matrix. We derive the cost for the optimal ratio $\frac{m}{d} = \frac{n}{c}$ below.

Using equation $P = c^2 d$ and $\frac{m}{d} = \frac{n}{c}$, solve for d, c in terms of m, n, P . Solving the system of equations yields $c = \left(\frac{Pn}{m}\right)^{\frac{1}{3}}, d = \left(\frac{Pm^2}{n^2}\right)^{\frac{1}{3}}$. We can plug these values into the cost of CA-CQR2 to find the optimal cost.

$$T_{\text{CA-CQR2}}^{\alpha-\beta}\left(m, n, \left(\frac{Pn}{m}\right)^{\frac{1}{3}}, \left(\frac{Pm^2}{n^2}\right)^{\frac{1}{3}}\right) = \mathcal{O}\left(\left(\frac{Pn}{m}\right)^{\frac{2}{3}} \log P \cdot \alpha + \left(\frac{mn^2}{P}\right)^{\frac{2}{3}} \cdot \beta + \frac{mn^2}{P} \cdot \gamma\right)$$

IV. EVALUATION

A. Implementation

The CA-CQR2 algorithm was implemented using modern C++. MPI [29] was used for all collective and point-to-point communication routines. BLAS [8] and LAPACK [30] were used as optimized implementations of sequential matrix multiplication and factorization routines. The implementation accounted for no overlap in computation and communication and a cyclic data distribution was used among processors.

The CFR3D algorithm provides constraints on the matrices CA-CQR2 can factor. For an $m \times n$ matrix A , n must be $2^k, k \in \mathbb{Z}$. Further, the tunable grid dimension d must be evenly divisible by c^2 . To illustrate, only five tunable grid shapes currently exist with 4096 processors: $(d, c) = (4096, 1), (1024, 2), (256, 4), (64, 8), (16, 16)$.

B. Experimental Setup

We ran experiments using the Blue Waters Cray XE6 supercomputer. Each Blue Waters XE node has two 16-core AMD 6276 Interlagos sockets. We used the MPICH and Cray LibSci implementations of MPI, BLAS and LAPACK, respectively. We operated in the Intel/5.2.82 environment, using the gcc 6.3.0 compiler with optimization flag -O3. All experiments were performed with 32 processes per node.

To provide an accurate comparison, we tested CA-CQR2 against the PGEQRF and PORQQR ScaLAPACK routines. For each problem size, we collected ScaLAPACK results over block sizes 1,8,16,32,64 and all possible 2D processor grid shapes. We collected CA-CQR2 results over all possible tunable grid shapes. We chose as data points results with the largest GFlops achieved. Note that we provide both effective and computed GFlops, the latter reflecting the fact that CholeskyQR2 performs $6mn^2 + n^3$ flops whereas ScaLAPACK PGEQRF performs $2mn^2 - \frac{2}{3}n^3$ flops.

C. Benchmarking results

We present strong and weak scaling results for a variety of problem sizes and provide a brief analysis. We test strong scaling by keeping the $m \times n$ matrix size constant and increasing the number of processors by powers of 8. We test weak scaling by keeping both the matrix size per processor and the leading-order flop cost constant. Specifically, we increase dimension m and p while keeping n and $\frac{m}{p}$ constant.

Figures 3(b) and 4(b) show that ScaLAPACK and CA-CQR2 achieve roughly the same peak performance when comparing the computed GFlop rates. Figures 3(a) and 4(a) show that ScaLAPACK outperforms CA-CQR2 when comparing the effective GFlop rates. Figure 3(a) illustrates that both ScaLAPACK and CA-CQR2 strong scale to 64 processors, but CA-CQR2 is a constant times less performant. Figure 3(b) illustrates that CA-CQR2 strong scales to 512 processors and achieves better absolute performance when considering

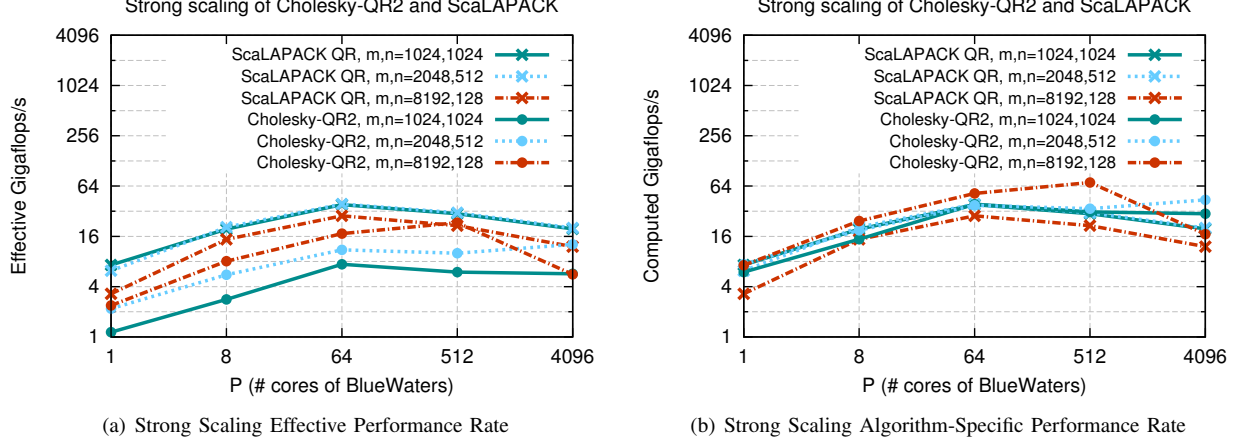


Figure 3: Peak performance for strong scaling experiments for various problem sizes m, n .

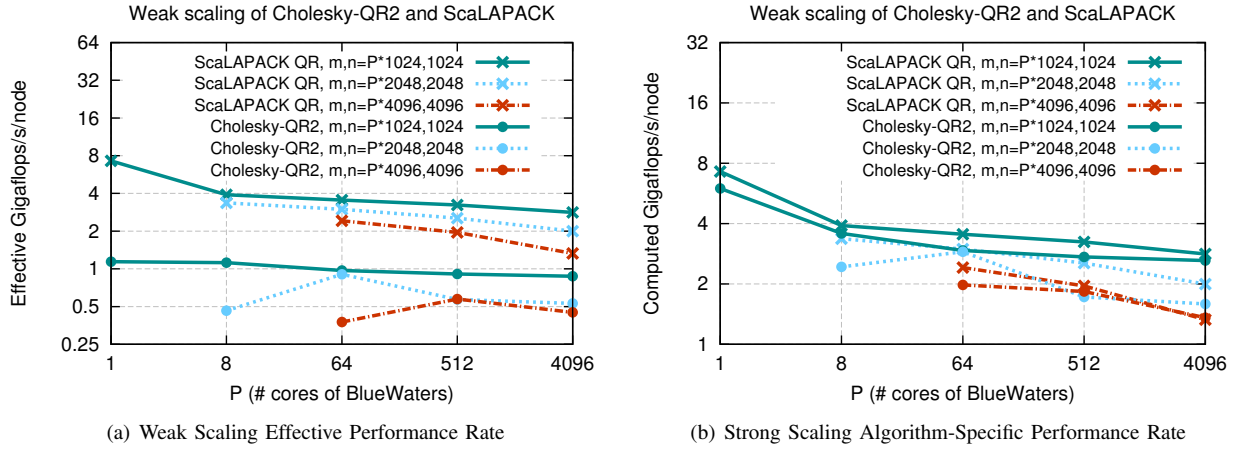


Figure 4: Peak performance for weak scaling experiments for various families of problem sizes $m = nP, n$.

the computed GFlop rate, but this might be reasoned by the difference in number of flops between the two algorithms.

Figure 4(a) shows that CA-CQR2 exhibits similar weak scaling characteristics to ScaLAPACK, yet achieves a constant less absolute performance. Figure 4(b) shows that when considering the computed GFlop rate, CA-CQR2 and ScaLAPACK achieve roughly the same absolute performance. Note that the communication cost improvement CA-CQR2 provides, a factor of $P^{\frac{1}{6}}$, will only become apparent when the problem size and number of processors grows. Thus, it is encouraging to see that for the largest problem size in figure 4(b), CA-CQR2 achieve the same performance as ScaLAPACK.

Figures 3(b) and 4(b) show that ScaLAPACK and CA-CQR2 achieve roughly the same peak performance when comparing the computed GFlop rates. Figures 3(a) and 4(a) show that ScaLAPACK outperforms CA-CQR2 when comparing the effective GFlop rates. Figure 3(a) illustrates that both ScaLAPACK and CA-CQR2 strong scale to 64 processors,

but CA-CQR2 is a constant times less performant. Figure 3(b) illustrates that CA-CQR2 strong scales to 512 processors and achieves better absolute performance when considering the computed GFlop rate, the former suggesting that an improvement due to CA-CQR2 performing a constant times more flops than Householder QR.

V. CONCLUSION

We have developed an algorithm that efficiently extends CholeskyQR2 (CQR2) to rectangular matrices. Through the use of a tunable processor grid, 1D-CQR2 has been generalized to a parallel algorithm equipped to efficiently factorize a matrix of any dimensions via an appropriate 3D algorithm variant. The regularity and simplicity, in combination with asymptotically optimal communication complexity, gives CA-CQR2 promising potential parallel QR factorization algorithm. In comparison to an optimized library, our implementation of CA-CQR2 generally performed worse by a factor proportional to the overhead in work of

CQR2 with respect to Householder QR. However, the CA-CQR2 algorithm matched the parallel scalability of a vendor-optimized implementation, and has promise due to its good theoretical communication complexity. Our research provides new insights to the communication complexity of CQR2 and the performance potential of parallel 3D QR algorithms.

One next step in this line of work is to further evaluate CFR3D to determine if its the most performant Cholesky factorization algorithm. Another is to evaluate more tunable grid shapes to provide a knob for lowering memory footprint. Further avenues include studying and improving the stability of CA-CQR in search for a rank-revealing algorithm variant. Developing a CA-CQR2 algorithm that operates on subpanels to reduce computation cost overhead is also of interest.

REFERENCES

- [1] T. Fukaya, Y. Nakatsukasa, Y. Yanagisawa, and Y. Yamamoto, "CholeskyQR2: A simple and communication-avoiding algorithm for computing a tall-skinny QR factorization on a large-scale parallel system," in *Proceedings of the 5th Workshop on Latest Advances in Scalable Algorithms for Large-Scale Systems, ser. ScalA '14*. Piscataway, NJ, USA: IEEE Press, 2014, pp. 31–38. [Online]. Available: <http://dx.doi.org/10.1109/ScalA.2014.11>
- [2] Y. Yamamoto, Y. Nakatsukasa, Y. Yanagisawa, and T. Fukaya, "Roundoff error analysis of the CholeskyQR2 algorithm," *Electronic Transactions on Numerical Analysis*, vol. 44, pp. 306–326, 2015.
- [3] G. Ballard, J. Demmel, L. Grigori, M. Jacquelin, H. D. Nguyen, and E. Solomonik, "Reconstructing Householder vectors from tall-skinny QR," in *Proceedings of the 2014 IEEE 28th International Parallel and Distributed Processing Symposium, ser. IPDPS '14*. Washington, DC, USA: IEEE Computer Society, 2014, pp. 1159–1170. [Online]. Available: <http://dx.doi.org/10.1109/IPDPS.2014.120>
- [4] J. Demmel, L. Grigori, M. Hoemmen, and J. Langou, "Communication-optimal parallel and sequential QR and LU factorizations," *SIAM J. Sci. Comput.*, vol. 34, no. 1, pp. 206–239, Feb. 2012. [Online]. Available: <http://dx.doi.org/10.1137/080731992>
- [5] A. Tiskin, "Bulk-synchronous parallel Gaussian elimination," *Journal of Mathematical Sciences*, vol. 108, no. 6, pp. 977–991, 2002. [Online]. Available: <http://dx.doi.org/10.1023/A:1013588221172>
- [6] —, "Communication-efficient parallel generic pairwise elimination," *Future Generation Computer Systems*, vol. 23, no. 2, pp. 179–188, 2007.
- [7] E. Solomonik, G. Ballard, J. Demmel, and T. Hoefer, "A communication-avoiding parallel algorithm for the symmetric eigenvalue problem," in *Proceedings of the 29th ACM Symposium on Parallelism in Algorithms and Architectures, ser. SPAA '17*. New York, NY, USA: ACM, 2017, pp. 111–121. [Online]. Available: <http://doi.acm.org/10.1145/3087556.3087561>
- [8] C. L. Lawson, R. J. Hanson, D. R. Kincaid, and F. T. Krogh, "Basic Linear Algebra Subprograms for Fortran usage," *ACM Transactions on Mathematical Software (TOMS)*, vol. 5, no. 3, pp. 308–323, 1979.
- [9] E. Chan, M. Heimlich, A. Purkayastha, and R. Van De Geijn, "Collective communication: theory, practice, and experience," *Concurrency and Computation: Practice and Experience*, vol. 19, no. 13, pp. 1749–1783, 2007.
- [10] R. Thakur, R. Rabenseifner, and W. Gropp, "Optimization of collective communication operations in mpich," *International Journal of High Performance Computing Applications*, vol. 19, no. 1, pp. 49–66, 2005.
- [11] J. Bruck, C.-T. Ho, S. Kipnis, E. Upfal, and D. Weathersby, "Efficient algorithms for all-to-all communications in multiport message-passing systems," *Parallel and Distributed Systems, IEEE Transactions on*, vol. 8, no. 11, pp. 1143–1156, 1997.
- [12] Y. Saad and M. H. Schultz, "Data communication in hypercubes," *Journal of Parallel and Distributed Computing*, vol. 6, no. 1, pp. 115 – 135, 1989. [Online]. Available: <http://www.sciencedirect.com/science/article/pii/0743731589900452>
- [13] J. L. Träff and A. Ripke, "Optimal broadcast for fully connected processor-node networks," *Journal of Parallel and Distributed Computing*, vol. 68, no. 7, pp. 887–901, 2008.
- [14] W. F. McColl and A. Tiskin, "Memory-efficient matrix multiplication in the BSP model," *Algorithmica*, vol. 24, pp. 287–297, 1999.
- [15] E. Dekel, D. Nassimi, and S. Sahni, "Parallel matrix and graph algorithms," *SIAM Journal on Computing*, vol. 10, no. 4, pp. 657–675, 1981.
- [16] R. C. Agarwal, S. M. Balle, F. G. Gustavson, M. Joshi, and P. Palkar, "A three-dimensional approach to parallel matrix multiplication," *IBM Journal of Research and Development*, vol. 39, pp. 575–582, September 1995.
- [17] A. Aggarwal, A. K. Chandra, and M. Snir, "Communication complexity of PRAMs," *Theoretical Computer Science*, vol. 71, no. 1, pp. 3 – 28, 1990.
- [18] J. Berntsen, "Communication efficient matrix multiplication on hypercubes," *Parallel Computing*, vol. 12, no. 3, pp. 335–342, 1989.
- [19] S. L. Johnsson, "Minimizing the communication time for matrix multiplication on multiprocessors," *Parallel Computing*, vol. 19, pp. 1235–1257, November 1993.
- [20] F. G. Gustavson, "Recursion leads to automatic variable blocking for dense linear-algebra algorithms," *IBM Journal of Research and Development*, vol. 41, no. 6, pp. 737–755, 1997.
- [21] A. George, M. T. Heath, and J. Liu, "Parallel Cholesky factorization on a shared-memory multiprocessor," *Linear Algebra and its applications*, vol. 77, pp. 165–187, 1986.
- [22] T. Wicky, E. Solomonik, and T. Hoefer, "Communication-avoiding parallel algorithms for solving triangular systems of linear equations," in *2017 IEEE International Parallel and Distributed Processing Symposium (IPDPS)*, May 2017, pp. 678–687.
- [23] D. P. O'Leary and P. Whitman, "Parallel QR factorization by Householder and modified Gram-Schmidt algorithms," *Parallel computing*, vol. 16, no. 1, pp. 99–112, 1990.
- [24] E. Elmroth and F. G. Gustavson, "Applying recursion to serial and parallel QR factorization leads to better performance," *IBM Journal of Research and Development*, vol. 44, no. 4, pp. 605–624, 2000.
- [25] J. Choi, J. J. Dongarra, L. S. Ostrouchov, A. P. Petit, D. W. Walker, and R. C. Whaley, "Design and implementation of the ScaLAPACK LU, QR, and Cholesky factorization routines," *Scientific Programming*, vol. 5, no. 3, pp. 173–184, 1996.
- [26] A. Buttari, J. Langou, J. Kurzak, and J. Dongarra, "Parallel tiled QR factorization for multicore architectures," *Concurrency and Computation: Practice and Experience*, vol. 20, no. 13, pp. 1573–1590, 2008.
- [27] M. Cosnard, J.-M. Muller, and Y. Robert, "Parallel QR decomposition of a rectangular matrix," *Numerische Mathematik*, vol. 48, no. 2, pp. 239–249, 1986.
- [28] E. Chu and A. George, "QR factorization of a dense matrix on a hypercube multiprocessor," *SIAM Journal on Scientific and Statistical Computing*, vol. 11, no. 5, pp. 990–1028, 1990.
- [29] W. Gropp, E. Lusk, and A. Skjellum, *Using MPI: Portable parallel programming with the message-passing interface*. Cambridge, MA, USA: MIT Press, 1994.
- [30] E. Anderson, Z. Bai, C. Bischof, J. Demmel, J. Dongarra, J. D. Croz, A. Greenbaum, S. Hammarling, A. McKenney, S. Ostrouchov, and D. Sorensen, *LAPACK Users' Guide*. Philadelphia, PA, USA: SIAM, 1992.